Effects of Crystal Selenium Nanoparticles (Cys Se-NPS) on Carbofuran-induced biochemical, immunohistochemical and ultrastructure changes in the Thyroid Follicles of Adult Male Albino Rats

Sahar Khalil[1], Omayma M Mahmoud[2], Hala M.F. Mohammad[3,4] and Abeer A. K. Mohamed[1]

Original Article

[1]*Department of Histology, Faculty of Medicine, Suez Canal University, Ismailia, Egypt*

[2]*Department of Human Anatomy and Embryology, Faculty of Medicine, Suez Canal University, Ismailia, Egypt*

[3]*Department of Clinical Pharmacology, Faculty of Medicine, Suez Canal University, Ismailia, Egypt*

[4]*Central Laboratory, Center of Excellence in Molecular and Cellular Medicine (CEMCM), Faculty of Medicine, Suez Canal University, Ismailia, Egypt*

ABSTRACT

Introduction: Carbofuran, a broad-spectrum carbamate insecticide (endocrine disruptor) affects thyroid glands. Selenium-NPs is effective as selenite as a trace element for thyroid gland functioning while being less hazardous.

Aim of wWork: The aim is to examine probable protecting effect of Cys Se-NPs on carbofuran induced rat thyroid glands damage.

Materials and Methods: Forty adult male albino rats were divided randomly to four groups; control group, carbofuran group: received 2.4 mg/kg bw carbofuran, carbofuran & Cys Se-NPs group: received carbofuran as previous group in addition to 0.3 mg/kg bw Cys Se-NPs and finally Cys Se-NPs group: received Cys Se-NPs. Serum analysis of T3 and, T4 hormones and tissue GSH and MDA markers were evaluated. Thyroid sections of 5 µm thickness were prepared for H&E stains, Masson's trichrome stains and detection of Ki67 antibodies immunohistochemical stain. Other thyroid specimens were processed for examination by transmission electron microscope.

Results: Carbofuran group significantly revealed reduction in GSH and both T3, T4 and increase level of MDA. Thyroid follicles were highly disorganized and destructed, with follicular cells stratification and significant increase in epithelial thickness. Exfoliated cells were detected in the colloid with reduction in its volume. Carbofuran & Cys Se-NPs group revealed significant rise in GSH and T3, T4 and reduction in MDA level. Histological and ultrastructure abnormalities were improved significantly. Ki67 index was reduced by 3.69% compared to 62.4% in carbofuran group.

Conclusions: Cys Se-NPs improved the changes induced by the toxic effects of carbofuran which can be a promising therapy against ROS produced by the carbofuran.

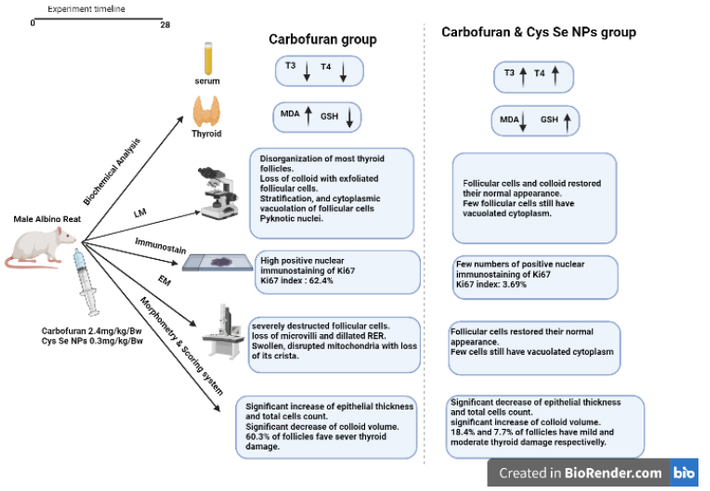

Graphical Abstract

 DOI: 10.21608/ejh.2022.155372.1751

Received: 09 August 2022, **Accepted:** 11 October 2022

Key Words: Carbofuran, cys se-nps, ki67 index, MDA&GSH, rat.

Corresponding Author: Sahar Khalil, MD, Department of Histology, Faculty of Medicine, Suez Canal University, Ismailia, Egypt, **Tel.**: +20 10 9889 2704, **E-mail:** saharkhalil@med.suez.edu.eg - skhalil7@yahoo.com

ISSN: 1110-0559, Vol. 46, No. 4

INTRODUCTION

Pesticides are the most common environmental contaminants that man and animals are exposed to through their manufacture, or during their usage in agriculture and domestic settings[1]. Pesticides effects include maximizing the crop yield, controlling vector-borne diseases, and preventing infestations that leads to improvement of quality of life. On the other hand, pesticides have toxic effects on the biological systems mainly in developing countries in which pesticide use is not controlled[2].

Carbofuran [2,3-dihydro-2, -2dimethyl-7 benzofuranol N-methylcarbamate], is carbamate broad-spectrum systemic pesticide used as household and agricultural pesticides in Egypt[3]. Carbamate pesticides are commonly substituted the more dangerous organophosphate pesticides due to its rapid degradation and relatively short residual life in the environment. In spite of these features, carbofuran residues was recounted in the ground, air, surface water, and food bringing about various toxic effects to the non-target organisms as humans[4]. These carbamates are known as endocrine disrupting pesticides affecting mainly the sex steroid and thyroid hormones. Their disrupting effects resulted from interference with production and/or activity of hormone such as inhibiting hormone synthesis, or binding directly to the receptors of hormone, or interfering breakdown of hormone[5].

Previously studies reported that carbofuran administration caused deterioration in cortisol levels, sex hormones without any effects on thyroid hormones. On the contrary, other studies stated that carbofuran affect the thyroid hormones through the histopathological changes it produced in the thyroid gland[5-7].

Selenium: a trace element that is essential for the thyroid gland as it articulates numerous particular selenoproteins that are concerned in metabolism of thyroid hormone and play a part as antioxidant defense[8]. There is extraordinary growth in nanotechnology research and its application in the diagnosis, treatment, and prevention of diseases as materials with its nanometer dimension display new properties different from those of both isolated atoms and bulk material. Nano-selenium (Se-NPs) particles produced a highly biological effective molecular compounds having unique characteristics. These characteristics are; the great surface area, elevated surface activity, high-level of catalytic efficacy, powerful adsorbing capability and the minimal toxicity[9].

The contradictory earlier studies result on carbofuran effect at the thyroid gland with the importance of the availability of selenium for the efficient functioning of the thyroid gland sparked our interest to examine the potential histopathological impact of carbofuran on thyroid gland. Additionally, earlier research has shown that Se-NPs is equally effective as selenite at upregulating levels of tissue Se and selenoenzymes, with less hazardous[10]. Therefore, this study aims at evaluating the postulated effect of Cys Se-NPs on rat's thyroid gland exposed to carbofuran administration.

MATERIAL AND METHODS

Experimental animals

Forty male adult albino rats (average weight 200-250g) brought from Faculty of Veterinary Medicine, Suez Canal University, Egypt. Animals were kept in well-ventilated wire mesh cages and put on a regular diet and water freely. For one week before any treatment, they kept beneath proper environments at room temperature with twelve-hour light/dark cycle for adaptation. This study was conducted following the Ethics of Research Committee of Faculty of Medicine, Suez Canal University, Ismailia, Egypt and with guide of National Institute of Health for care and usage of research laboratory animal (NIH Publication No. 8023, revised 1978). All needed precautions were taken to reduce animals' suffering to the utmost extent possible.

Chemicals

Carbofuran (98% purity): white powder was bought from Sigma-Aldrich Corp St. Louis, USA. It was dissolved in distilled water. Rats received 2.4 mg/kg body weight; equivalent to 17% of the Carbofuran mean lethal dose (oral LD50 of 8–14 mg/kg in rats)[11]

Selenium nanoparticles: crystal nano-selenium particles (Cys Se-NPs) suspension, sphere like shape (20-50 nm particle size) were brought from Nano-tech Lab, 6th October City, Egypt, as it was dissolved in phosphate buffered saline (PBS). Characterization of Cys Se-NPs particles shape and size was done by transmission electron microscopy (Figure 1).

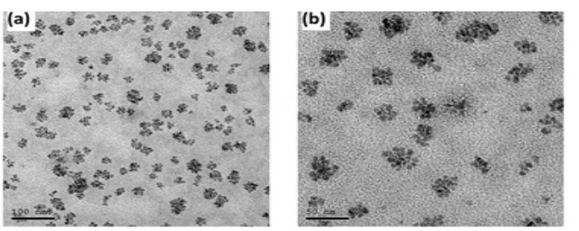

Fig. 1: Transmission electron microscopy of cys Se-NPs shows their shape and size

Experimental designs

Animals were randomly divided into four group (10 animals/each) and all treatments were given by gastric intubation, once daily for 28 days.

Group 1 (control group): This group included two equivalent subdivisions

- Subgroup 1a: animals hadn't been given any treatment.
- Subgroup 1b: animals received 5ml/kg body weight Phosphate Buffer Saline (PBS) (Sigma-Aldrich Corp St. Louis, USA).

Group 2 (carbofuran group): Animals received carbofuran (2.4 mg/kg bw)[4].

Group 3 (carbofuran & Cys Se-NPs group): Animals received carbofuran in the same dose as group 2 concurrently with Cys Se-NPs (0.3 mg/kg bw)[12].

Group 4 (Cys Se-NPs group): Animals received Cys Se-NPs at the same dose as group 3.

Just before scarification by decapitation, the rats were anesthetized by [60 mg/kg ketamine and 5 mg/kg xylazine] intraperitoneally. The tissues of thyroid glands were excised, and each gland was divided longitudinally into two parts; the right part was used to perform the histopathological, immuno-histochemical and transmission electron microscopic samples. Left part was isolated in ice cold PBS to prepare tissues homogenates for evaluation of tissue oxidative and antioxidants markers.

Biochemical Analysis

Blood samples from retro orbital vein were collected 24 hours after the last dose of both carbofuran and Cys Se-NPs and serum was prepared and stored at −20 °C until used for analysis of thyroid-stimulating hormone (TSH), free triiodothyronine (T3), and free thyroxine (T4) hormones. Quantitative analysis of these hormones was performed by enzyme-linked immunosorbent assay (ELISA). The data were expressed as ng/ml for T3 and T4, and as pg/ml for TSH.

Tissue collection and preparation for oxidative and antioxidant analysis

A sample of the thyroid gland was rinsed with ice- PBS and at once frozen using liquid nitrogen and kept at −80 °C pending analysis of the potent antioxidant glutathione (GSH) and the oxidative stress marker malondialdehyde (MDA) using high-performance liquid chromatography (HPLC) and fluorometric detection. Both GSH and MDA were reported as mmol/g tissue[13]. The biochemical, oxidative and antioxidative analysis were done in Biochemistry Department, Faculty of Medicine, Suez Canal University.

Histopathological Studies

Light microscopic assessment: Samples fixed in 10% neutral-buffered formaldehyde solution for 24 hours, later dehydrated and implanted into paraffin wax to form 5 µm thickness paraffin sections and stained by Hematoxylin and Eosin (H&E) stain, and Masson's trichrome stain[14].

Immunohistochemical examination

Ki67 antibodies immunohistochemical staining was used for detection of cellular proliferation. Paraffin sections were deparaffinized, rehydrated and pre-treated for retrieval of antigen in addition to buffer of sodium citrate (pH 6.0) for (20-30 min). Then sections have being incubated with monoclonal anti-Ki67 antibody (ab16667) (abcam plc, Cambridge, UK) (dilution range 1:200) for 1 hour. To be quite sure, negative control sections were run as routine with avoiding addition of primary antibody. The primary antibody has been identified using (IgG H&L (HRP) ab6721 of Goat Anti-Rabbit) (abcam plc, Cambridge, UK). DAB was used as Chromogen (1–2 min) then counterstained of slides were done by Harris's hematoxylin, then dried and covered. Dark-brown nucleus color in addition to a granular configuration was expressed as positive reaction (for positive control, tonsil was used).

Transmission electron microscopic examination: Specimens (1 mm3) have been fixed with solution of 2.5% glutaraldehyde at 4°C for 24 hours, then post-fixation done for one hour in osmium tetroxides (2%), then dehydration and resin embedding were done. Cutting the semi-thin sections were done by ultramicrotome, then stained by toluidine blue stain and assessed with light microscope. Ultrathin sections have being cutting then stained by uranyl acetate and lead citrate[15]. Examination of the grids and photographed by using Transmission Electron Microscope (JEOL-EX 1010 TEM), Faculty of Science, Ain Shams University, Egypt.

Histopathological assessment

Thyroid follicles were histo-pathologically evaluated in 30 thyroid follicles per animal in non-overlapping fields x40 in H&E-stained sections. The parameters were scored from 0 to 3 (for each parameter): abnormal thyroid follicular cell proliferation (hyperplastic follicle), desquamated epithelium into follicular cavity, colloid alterations (in the form of vacuolations, varying quantities, and/or entire disappearance), vascular congestion.

Additionally, the presence of interstitial collagen deposits was evaluated in the Masson's trichrome stained sections[16].

(Table 1) displays the degree of changes for each score from 0 to 3. Final score for thyroid gland damage were calculated (Table 2)

Table 1: Parameters of histopathological scoring system for the thyroid gland damage

Scoring system for each parameter	Parameter				
	Hyperplastic follicle	Vascular Congestion	Colloid changes in form of vacuolations, variable amount, and/or total disappearance	Desquamated epithelium	Interstitial collagen deposits
0	Normal morphology				
1	Changes present in <10% of the follicular cavities				
2	Changes present in 10-40% of the examined follicles				
3	Changes present in >40% of the examined follicles				

Table 2: Final histopathological score of thyroid gland damage

	Normal (0-3)	Mild (4-6)	Moderate (7-9)	Severe (10-12)
Control group	100%	0	0	0
carbofuran group	0	10%	30%	60%
carbofuran & cys Se NPs group	70%	20%	10%	0
cys Se NPs group	100%	0%	0%	0

The following quantitative measurements were done by Fiji-image J software program[17].

1. The mean follicular cell (epithelial) thickness was measured by choosing four epithelial cells at 12, 3, 6 and 9 o'clock position for 30 follicles/each animal.
2. Calculation of colloid volume.
3. Total follicular (epithelial) cell count.
4. Calculation of the Ki67 index by counting the number of positively stained Ki67 cells/total number of cells ×100.
5. Nuclear/cytoplasmic (N/C) ratio.
6. The collagen fiber optical density deposits using Masson's trichrome stain. (Table 3)

Table 3: Morphometrical parameters of the thyroid glands of the studied groups

	control group (mean± SD)	carbofuran group (mean± SD)	Carbofuran & cys Se-NPs group (mean± SD)	cys Se-NPs group (mean± SD)	*F value*
Epithelial thickness	3.69±0.6	8.97 ± 2.8^{a}	$7.2\pm1.4^{a,b}$	3.63 ± 0.6^{b}	104.24
Colloid Volume	$27.4\pm6.8x10^{4}$	$2.5\pm2.9x10^{4a}$	$10.98\pm5.1x10^{4a,b}$	$26.04\pm5.5x10^{4b}$	52.5
Total cell counts	223.8±13.6	281.7 ± 32^{a}	248.6 ± 34.1^{b}	226.2 ± 14.8^{b}	11.15
Positive Ki67cells count	0.6±0.69	175.9 ± 27.02^{a}	8.8 ± 3.2^{b}	0.6 ± 0.7^{b}	402.5
Ki67 index	0.27%	62.4%	3.69%	0.26%	------
N/C	0.16±0.01	0.11 ± 0.02^{a}	0.09 ± 0.01^{a}	0.16 ± 0.01^{b}	39.83
The optical density of collagen fiber	117.2±5.5	182.6 ± 11.7^{a}	$141.9\pm 12.6^{a,b}$	116.7 ± 4.7^{b}	110.11

One way ANOVA and Post hoc (Tukey) test was used. Statistically significant at $p<0.05$.
a significant compared to control group b significant compared to carbofuran group

Statistical analysis

The collected biochemical and morphometric data expressed the same as mean ± standard deviation (SD). Statistics were managed using one-way (ANOVA) analysis of variance test of SPSS 5 (SPSS Inc., Chicago, IL, USA) and followed by "Tuckey" post hoc significant difference. Results were regard as significant statistically when *P value* was ≤0.05.

RESULTS

General observation

During the experiment, there were no rats' deaths, no differences in the appearance and behavior of Cys Se-NPs and carbofuran groups compared to the control one.

Biochemical analysis

Thyroid hormones

The current study revealed a significant reduction in mean± SD of free T3 and T4 levels (80.20±4.158 and 2.581±0.2282 respectively) (F 141.62 and 176.37 respectively) ($P<0.05$) of carbofuran group in comparison with control group (123.20±7.671 and 4.69 ±0.0727), carbofuran & Cys Se-NPs group (91.40±3.2042 and 3.232±0.4334), and Cys Se-NPs group (124.60±7.5011 and 4.667 ± 0.0904) (Figure 2).

TSH results shows non-significant statistically variation between all investigated groups (results not shown).

MDA and GSH levels

Statistically significantly increase of mean±SD of MDA

level (12.41±1.81) (F 38.7) (P<0.05) in the carbofuran group in comparison with control group were recorded. Meanwhile, there was significant decrease in carbofuran & Cys Se-NPs group (9.21±1.07), and Cys Se-NPs group (7.59±0.91) compared to carbofuran group (Figure 3A).

In terms of GSH level, there was a significant decrease in mean ± SD (15.30±3.31) (F 354.5) in the carbofuran group in comparison with control group. While a significantly increase in carbofuran & Cys Se-NPs group (119.87±9.04), and Cys Se-NPs group (82.57±7.52) compared to carbofuran group also recorded (Figure 3B)

Light microscopic examination: sections of both H&E stain and toluidine blue semithin of thyroid glands of the control and Cys Se-NPs groups showed normal thyroid structure. Sections of both have many follicles of various sizes separated by connective tissue and blood vessels. Simple cuboidal epithelium (follicular cells) with (3.69±0.64 and 3.63±0.64) thickness respectively bordered the central acidophilic homogeneous colloid-filled lumen of each follicle (colloid volume 27.4±6.79x10^4, 26.04±5.51x104, respectively). The total epithelial cell count was 223.8±13.55 and 226.2±14.8 respectively. The follicular cells had central spherical vesicular nuclei with prominent nucleoli (Figure 4a). The nuclear/cytoplasmic ratio was 0.16±0.008 and 0.16±0.008 respectively (Table 3). Histopathological scoring of these groups was 100% normal (0-3) (Table 2). In semithin sections colloid appeared homogeneous with no vacuolations (Figure 5a).

Regarding carbofuran group, thyroid gland sections showed disorganization of most of the thyroid follicles, loss, or tiny amount of colloid was significantly reduced in comparison with control. In the lumen of the thyroid follicles, exfoliated follicular cells were seen. There was also stratification of the follicular cells (total epithelial cell count and epithelial thickness were significantly increased compared to control) with vacuolated cytoplasm and pyknotic nuclei (N/C ratio was significantly decreased compared to control). Congested dilated blood vessels are apparent at interfollicular tissues (Figures 4 b,c) (Table 3). Histopathological scoring was 60% severe, 30% moderate and 10% mild (Table 2). In semithin sections, some follicles had disrupted colloid of varying quantities and densities. Vacuolated colloid found in several follicles. The presence of enlarged parafollicular cells was noticed in some sections (Figures 5 b,c).

Alternatively, examination of thyroid gland sections of carbofuran & Cys Se-NPs group revealed improvement of the histopathological alterations of the thyroid glands, most of the follicular cells (total epithelial cell count and epithelial thickness were significantly decreased compared to carbofuran group) and colloid were restored to their normal appearance (was significantly increased compared to carbofuran group). However, there were still a few follicular cells with vacuolated cytoplasm (Figure 4d) (Table 3). Histopathological scoring of was 70% normal, 20% mild and 10% moderate (Table 2). In semithin sections, follicles were filled with colloid of various densities. Nearly normal parafollicular cells were also identified (Figure 5d).

Masson's Trichrome stained sections: The collagen was minimally detected in the interstitial tissue in sections of both the control and Cys Se-NPs groups stained with Masson's trichrome (Figure 6a). In contrast, collagen deposition increased in the carbofuran group (Figure 6b), with thickened collagen fiber in between the follicles, as compared to the control. Carbofuran & Cys Se-NPs group showed little amount of collagen compared to carbofuran group (Figure 6c) (Table 3).

Immunohistochemical examination of Ki67 as a cellular proliferation marker

Control and Cys Se-NPs groups thyroid gland examination showed Ki67-negative nuclei (Figure 7a). However, a high proportion of follicular cells in the carbofuran group displayed positive nuclear immunostaining in form of brown nuclear deposits (Figure 7b). Nuclei in the carbofuran & Cys Se-NPs group had fewer number of positive nuclear immunostaining than those in the carbofuran group (Figure 7c) (Table 3).

Transmission electron microscopic results

Ultrathin sections of the control and Cys Se-NPs groups thyroid glands follicles showed that each follicle lined with a one layer of euchromatic nuclei cuboidal follicular cells, regular and well-formed nuclear membrane, and prominent nucleolus. Multiple mitochondria, a well-formed rough endoplasmic reticulum (RER), lysosomes and prominent Golgi complex, seen in their cytoplasm. Short microvilli protruded from the apical surface of the follicular cells in the lumen, which was filled by relatively dense colloid (Figures 8 a,b). There were also para follicular cells (PF) with euchromatic nuclei, large nucleoli, and blood vessels, as well as a thin basement membrane that support the follicular cells (Figure 8c).

The thyroid glands of carbofuran group revealed obvious changes in the follicular cells. Some follicles showed evident stratification of the follicular cells. Many thyroid follicles had destructed follicular cells with distorted flat heterochromatic nuclei, significantly vacuolated cytoplasm, and partially lost microvilli on the apical surface. There were also parafollicular cells with dark shrunken nuclei and congested blood vessels (Figure 8d). Variable degrees of dilated RER were the most significant cytoplasmic ultrastructural characteristic of follicular cells. Swollen mitochondria with disrupted or even lost cristae were also seen, as well as an evident increase of follicular cells lysosomal content (Figures 8 d,e). Many thyroid follicles had thick irregular basement membranes, vacuolated colloid, and desquamated follicular cells (Figure 8 f,g).

The Carbofuran & Cys Se-NPs treated group demonstrated nearly restoration of normal thyroid follicular

cells structure with euchromatic nuclei, well-formed nuclear membrane with apical microvilli projecting to colloidal lumen which contain small vacuole. The follicular cells cytoplasm has numerous paralleled cisternae of normal rough endoplasmic reticulum, mitochondria, and dense lysosomal granules (Figures 8 h,i).

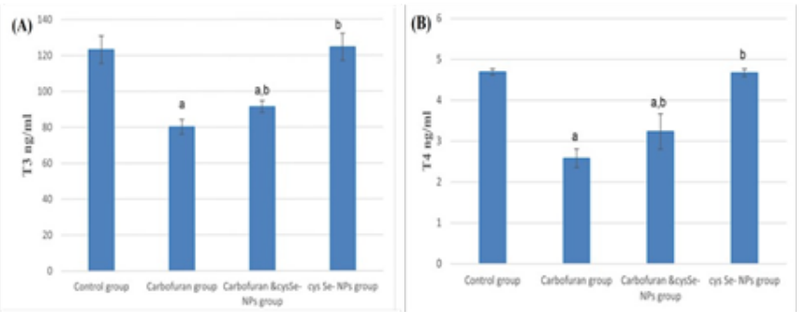

Fig. 2: Thyroid hormones levels among studied groups; (A) T3 level, and (B) T4 level. Results shown as mean ± SD and analyzed using one-way ANOVA followed by post-hoc Tukey's HSD test. *P*<0.05. a significant compared to control, b significant compared to carbofuran group

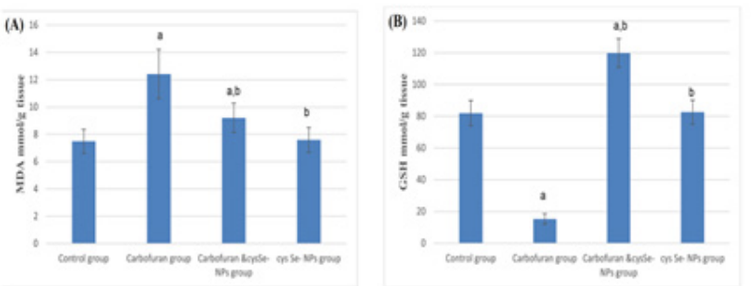

Fig. 3: The levels of MDA and GSH levels among studied groups. Results shown as mean ± SD and analyzed using one-way ANOVA followed by post-hoc Tukey's HSD test. *P*<0.05. a significant compared to control, b significant compared to carbofuran group

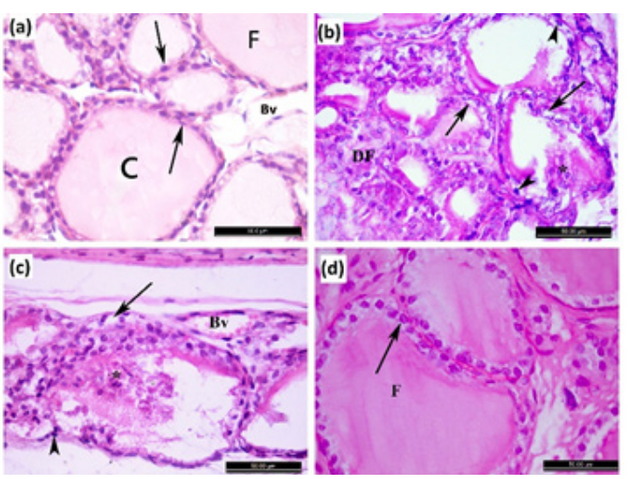

Fig. 4: Photomicrographs of sections in the thyroid gland of: (a) control group showing various sized thyroid follicles (F), lined by follicular cuboidal epithelial cells (arrow), filled with lightly stained colloid (C), separated by interfollicular blood vessels (Bv). (b) Carbofuran group showing disrupted follicles (DF), some follicles devoid of colloid or contain small amount, desquamated cells in the lumen of follicle (*), pyknotic follicular nuclei (arrowhead) and some follicular cells with vacuolated cytoplasm (arrow). (c) Carbofuran group showing stratification of the follicular cells with vacuolated cytoplasm (arrow) and pyknotic nuclei (arrowhead), congested and dilated blood vessel (Bv), desquamated cells in the lumen of follicle (*). (d) Carbofuran & cys Se-NPs group showing thyroid follicle (F), lined by follicular epithelium (arrow). (H&E x650)

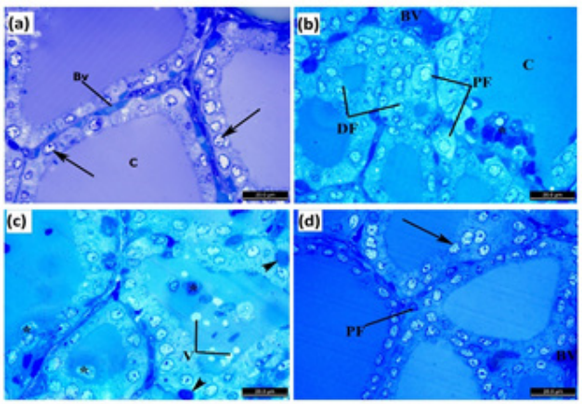

Fig. 5: Photomicrographs of sections in the thyroid gland of: (a) control group showing thyroid follicle lined by cuboidal epithelium (arrow), filled with colloid (C) surrounded by blood vessels (Bv). (b) Carbofuran group showing thyroid follicle with disrupted follicular cells (DF) and small colloidal space, congested and dilated blood vessel (BV), desquamated cells (*) in the colloidal lumen of follicle (C). notice also the enlarged parafollicular cells (PF). (c) Carbofuran group showing thyroid follicles with desquamated cells (*) in the colloidal lumen, and vacuolation of colloid (V). Pyknotic nuclei of follicular cells are seen (arrowhead). (d) Carbofuran & cys Se-NPs group showing thyroid follicle lined by cuboidal epithelium (arrow), filled with colloid surrounded by blood vessels (BV). Notice the parafollicular cell (Toluidine bule x1000)

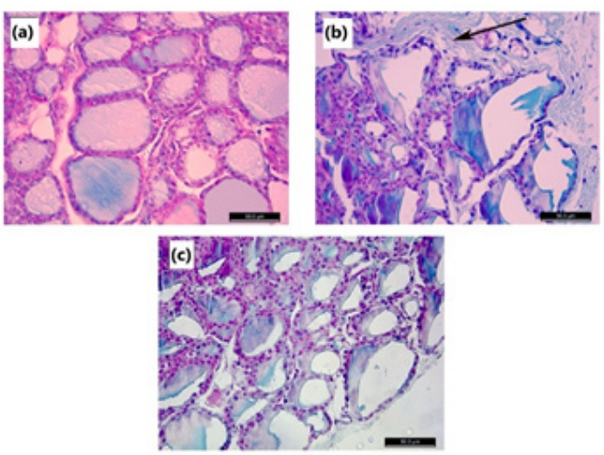

Fig. 6: Photomicrographs of sections in the thyroid gland of: (a) control group showing minimal amount of collagen deposition present within the gland. (b) Carbofuran group showing thickened collagen fibers in between the follicles (arrow). (c) Carbofuran & cys Se-NPs group showing little amount of collagen deposition. (Masson's trichrome x400)

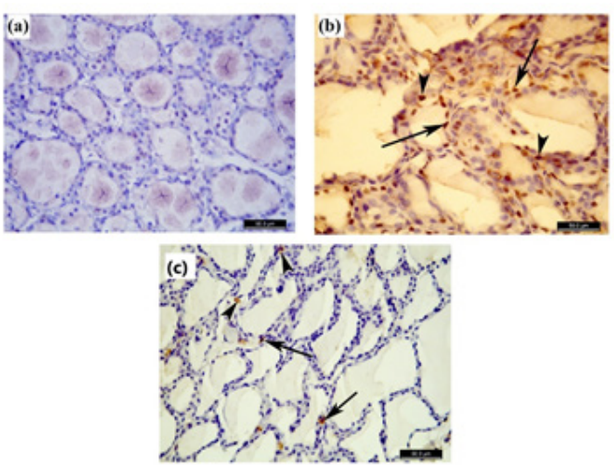

Fig. 7: Photomicrographs of sections in the thyroid gland of: (a) control group showing negative nuclear immune reaction of Ki67. (b) carbofuran group showing Ki67 positive immunoreaction in the form of brown nuclear deposits in many follicular (arrow) and parafollicular cells (arrowhead). (c) carbofuran & cys Se-NPs group showing few positive follicular cells for Ki67 immunostaining (arrow) and parafollicular cells (arrowhead). (Ki67 immunostaining x400)

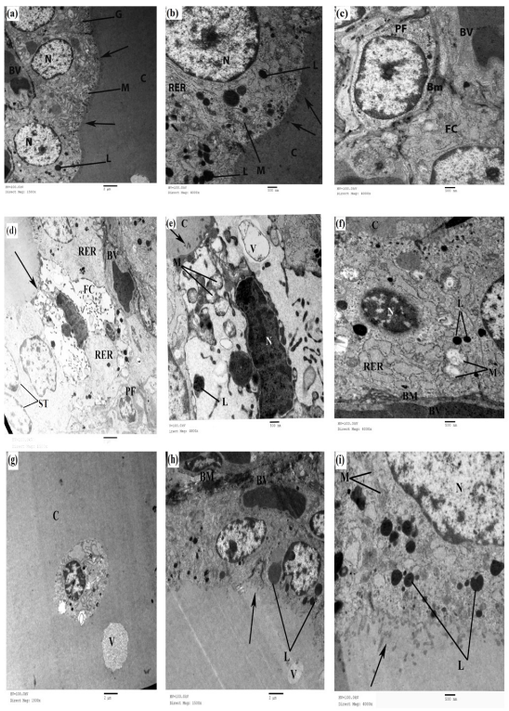

Fig. 8: An electron photomicrograph of ultrathin section in the thyroid gland of control group (a-c) showing (a) part of thyroid follicle. The follicular cells with euchromatic nuclei (N), the apical border with microvilli (arrow), projecting to colloidal lumen (C), mitochondria (M), dense lysosomal granules (L), prominent Golgi complex (G) and blood vessel are also shown (BV). (b) follicular cells contain euchromatic nucleus (N) with regular and well-formed nuclear membrane and prominent nucleolus. The cytoplasm has numerous parallel cisternae of normal rough endoplasmic reticulum (RER), longitudinal mitochondria (M), dense lysosomal granules (L), The cell showed the apical border microvilli (arrow) projecting into colloid lumen. (c) para follicular cell (PF) with euchromatic nucleus and prominent nucleolus (N). Basement membrane (BM) that form the base of the follicular cell (FC), and Blood vessels (BV).
Carbofuran group (d-g): showing (d) stratification of the follicular cells (ST), destructed follicular cell (FC) with distorted flat heterochromatic nucleus, the cytoplasm is markedly vacuolated, and the apical surface shows partially lost microvilli (arrow). The other cells have markedly dilated rough endoplasmic reticulum (RER). Notice the dark shrunken nucleus of parafollicular cell (PF) and congested blood vessel (BV). (e) markedly destructed follicular cell with distorted heterochromatic nucleus, the cytoplasm is markedly vacuolated (V), mitochondria are destructed, swollen with loss of cristae (M) and many lysosomes (L), the apical surface shows partially lost microvilli (arrow) into colloidal lumen (C). (f) markedly shrunken nucleus (N), swollen destructed mitochondria, with loss of its cristae (M), many lysosomes (L), markedly dilated rough endoplasmic reticulum (RER), congested blood vessels (BV) and irregular thick basement membrane (BM). (g) colloidal space with desquamated cells (*) and vacuolation (V).
Carbofuran & cys Se-NPs treated group (h&i) showing (h) nearly normal follicular cells with euchromatic nuclei, apical border with microvilli (arrow) projecting to the colloidal lumen which contains small vacuole (V), dense lysosomal granules (L), basal membrane (BM) and blood vessel (BV). (i) follicular cell contains euchromatic nucleus (N) with regular and well-formed nuclear membrane. mitochondria (M), dense lysosomal granules (L), apical border microvilli (arrow) projecting into the colloid lumen. ((a) 1500x, (b) 4000x, (c) 4000x, (d) 1500x, (e) 4000x, (f) 4000x, (g) 1500x, (h) 1500x, (i) 4000x)

DISCUSSION

The current study found that carbofuran exposure resulted in thyroid gland hypofunction and thyroid tissue damage. The Carbofuran group significantly exhibited reduction of free levels of both T3 and T4, reduced GSH level, with significant increase of MDA level in comparison to control. These findings are consistent with other researchers who discovered that carbamate produced hypothyroidism in rats by reducing thyroid iodine uptake, serum protein bound iodine, T3, T4 and the activity of thyroid peroxidase[18,19]. These thyroidal changes could be explained by the observation that carbamates cause thyroxine excretion from liver to be accelerated, the level of serum free T4 falls because of this acceleration[20]. Carbofuran may alter the synthesis and secretion of T3 and T4, based on the reduction of serum levels of this hormone of carbofuran group. TSH level, in contrast, showed no significant difference between the studied groups which is in agreement with another study which used different doses of carbofuran on male rats (0.6, 1.2, and 2.4 mg/ kg bw) and found no significant differences between groups[5].

In agreement with the current study many authors found that carbofuran administration produced a significant increase in malonaldehyde (MDA) levels in both human and animal species. These results can be explained by that carbofuran exposure could be related to rise in reactive oxygen species ROS generation these in turn led to elevated MDA level[21,22]. GSH is the first line defense against cellular damage caused by (ROS) some researcher explained that diminished GSH levels could be due to its consumption in countering the prevailing oxidative stress caused by ROS generated from carbofuran oxidative stress[7,23]. These findings showed that carbofuran had the ability to change the oxidative-antioxidative balance which agree with present study results.

The histopathological results of carbofuran group in this study revealed that, most of thyroid follicles (60%) were severely disorganized and destructed. Stratification of the follicular cells with significant increase of epithelial thickness and total cell count were seen. Cytoplasmic vacuolation and swollen disrupted mitochondria with loss of cristae also found. Most of the nuclei were pyknotic with distorted flat heterochromatin. There was a significant decrease of colloid volume and some follicles showed total loss of colloid with exfoliated follicular cells. These findings matched as well as those of other authors who found that carbofuran has a harmful effect on male rats' thyroid glands. Authors reported, after 28 days of exposure to oral carbofuran, alteration in follicular architecture, resulted in inactive follicles, reduced colloid resorption, and a decrease in serum thyroxine (T4) levels[4]. Furthermore, hypothyroidism is thought to be the cause of the higher incidence of hyperplastic and abortive follicles in the intervention group. The low level of thyroxine in the blood may activate the pituitary thyroid axis' negative feedback mechanism, causing it to produce more thyroid stimulating hormone, resulting in hyperplasia. A previous study found that rats exposed to goitrogenic substances such insecticides had thyroid hyperplasia with abortive follicles[24].

Se nanoparticles have recently been discovered to show antioxidant properties. In this study Cys-Se NPs administration significantly revealed reduction in MDA and increase of GSH in comparison to carbofuran group. These results were in agreement with many studies which recognized that using the Se-NPs was further effective than ionized selenium (Ise) in reducing the unwanted side effects of Bisphenol A (BPA). It has concerned a widespread courtesy because of its extreme bioavailability, low-slung toxicity, with antioxidant action. These effects said to be achieved through enhancing glutathione activity and reducing oxidative stress. The use of Cys-Se NPs in rats appeared to prevent thyroid damage. This was demonstrated by the recovery of serum free T3 and T4 levels, together with thyroid antioxidant activity, as measured with the concentrations of GSH and MDA, to near-normal levels[24].

Emara, 2019 compared nano-selenite (Nano-Se) effects with sodium selenite (SSe) of T3 and T4 serum levels and came to the same conclusion. He concluded that Nano-SE was more successful in raising thyroid hormone than SSe[25].

Thyroid gland histological and ultrastructure abnormalities improved significantly with the addition of Cys-Se NPs. Many follicles (70%) showed normal cubical follicular epithelium and were filled with homogeneous eosinophilic colloid material with no lack’s vacuoles. The Ki67 index was reduced by 3.69% compared to 62.4% in the carbofuran group, showing lower-level stratification and restoration of normal follicular thickness. These findings matched with other studies who observed that despite the presence of congested blood capillaries, Se nanoparticles treatment resulted in near-normal follicular shape[26,27].

Ki67 could be a useful marker for determining the aggressiveness of tumors and inflammatory lesions. Furthermore, rats' thyroids had slightly collagen deposition with little Ki67-stained nuclei[28].

In conjunction with earlier studies, the current study hypothesizes that Cys-Se NPs influences the immune system's response to thyroid gland alterations and protect follicular cells from oxidative damage produced by carbofuran exposure, which resulted in thyroid damage and fibrosis. Selenium supplementation has been shown to improve glutathione peroxidase (GPx) and other selenoprotein activities[29,30].

CONCLUSION

The use of nano-selenium (50-100 nm) counteract carbofuran toxicity has yielded a promising novel therapeutic regenerative material against ROS caused by carbofuran. The administration of selenium nanoparticles had a positive impact on the biochemical, histological, and ultrastructural changes that occurred in thyroid after exposure to carbofuran.

HIGH LIGHT

- Cys Se-NPs significantly increase the level of GSH.
- Cys Se-NPs significantly increase the level of both T3, T4 hormones
- Cys Se-NPs significantly decrease the level MDA.
- Cys Se-NPs Enhances histological and ultrastructure thyroid abnormalities
- Cys Se-NPs significantly reduced Ki67 index.

STATEMENT OF ETHICS

This study procedure was examined and authorised by the Faculty of Medicine, Suez Canal University, Egypt's Research Ethics Committee, and they follow the National Institutes of Health's standard for the care and use of laboratory animals (NIH Publications No. 8023, revised 1978). There was a concerted attempt to reduce animal suffering and the number of animals employed. All of the data from the experiments was examined in a blinded manner.

FUNDING SOURCES

Grant funding was not available for this study. The authors paid for all sources used in the creation of the data in this study.

CONFLICT OF INTERESTS

There are conflicts of interest.

REFERENCES

1. Kim, K.-H., E. Kabir, and S.A. Jahan, Exposure to pesticides and the associated human health effects. Science of The Total Environment, 2017. 575: p. 525-535https://doi.org/10.1016/j.scitotenv.2016.09.009 DOI|.

2. Van Dyk, J.S. and B. Pletschke, Review on the use of enzymes for the detection of organochlorine, organophosphate and carbamate pesticides in the environment. Chemosphere, 2011. 82(3): p. 291-307https://doi.org/10.1016/j.chemosphere.2010.10.033 DOI|.
3. El-Wakeil, N., *et al*., Pesticide-residue relationship and its adverse effects on occupational workers. 2013: p. 57-81
4. Hadie, S.N.H., O. Mansor, and S.E.T. Shariff, The effect of carbofuran on thyroid gland of male rats. International Medical Journal, 2012. 19(1): p. 16-20
5. Hadie, S.N.H., *et al*., Effects of Carbofuran on Thyroid Stimulating Hormone in Sprague-Dawley Rats. International Medical Journal, 2013. 20(2): p. 177-180
6. Boas, M., K.M. Main, and U. Feldt-Rasmussen, Environmental chemicals and thyroid function: an update. Current Opinion in Endocrinology, Diabetes and Obesity, 2009. 16(5): p. 385-391
7. Ibrahim, B.A., *et al*., Chronic Pesticides Exposure and Thyroid Functions among Farmers in Almnaif District-Ismailia Governorate, Egypt. Suez Canal University Medical Journal, 2020. 23(2): p. 117-128
8. Drutel, A., F. Archambeaud, and P. Caron, Selenium and the thyroid gland: more good news for clinicians. Clinical endocrinology, 2013. 78(2): p. 155-164
9. Hassanin, K.M., S.H. Abd El-Kawi, and K.S. Hashem, The prospective protective effect of selenium nanoparticles against chromium-induced oxidative and cellular damage in rat thyroid. International journal of nanomedicine, 2013. 8: p. 1713
10. Zhang, J., *et al*., Comparison of short-term toxicity between Nano-Se and selenite in mice. Life Sciences, 2005. 76(10): p. 1099-1109https://doi.org/10.1016/j.lfs.2004.08.015 DOI|.
11. Berny, P., Pesticides and the intoxication of wild animals. Journal of veterinary pharmacology and therapeutics, 2007. 30(2): p. 93-100
12. Rezaeian-Tabrizi, M. and A. Sadeghi, Plasma antioxidant capacity, sexual and thyroid hormones levels, sperm quantity and quality parameters in stressed male rats received nano-particle of selenium. Asian Pacific Journal of Reproduction, 2017. 6(1): p. 29
13. Yadav, Y.C., Effect of cisplatin on pancreas and testes in Wistar rats: biochemical parameters and histology. Heliyon, 2019. 5(8): p. e02247https://doi.org/10.1016/j.heliyon.2019.e02247 DOI|.
14. Layton, C., J.D. Bancroft, and S.K. Suvarna, 4—Fixation of tissues. Bancroft's Theory and Practice of Histological Techniques, 8th ed.; Suvarna, SK, Layton, C., Bancroft, JD, Eds, 2019: p. 40-63
15. Brydson, R., *et al*., Analytical transmission electron microscopy. Reviews in Mineralogy and Geochemistry, 2014. 78(1): p. 219-269
16. Vasiliu, I., *et al*., Protective role of selenium on thyroid morphology in iodine-induced autoimmune thyroiditis in Wistar rats. Exp Ther Med, 2020. 20(4): p. 3425-343710.3892/etm.2020.9029 DOI|.
17. Schindelin, J., *et al*., Fiji: an open-source platform for biological-image analysis. Nature Methods, 2012. 9(7): p. 676-68210.1038/nmeth.2019 DOI|.
18. Slotkin, T.A., *et al*., Does thyroid disruption contribute to the developmental neurotoxicity of chlorpyrifos? Environmental Toxicology and Pharmacology, 2013. 36(2): p. 284-287https://doi.org/10.1016/j.etap.2013.04.003 DOI|.
19. Mohamed, H.K. and A. Rateb, Histoloical and Biochemichal Study on the Toxic Effects of Bisphenol A on the Thyroid Gland of Adult Male Albino Rats and the Possible Protection by Selenium %J Egyptian Journal of Histology. 2019. 42(3): p. 667-68510.21608/ejh.2019.6757.1055 DOI|.
20. Hosokawa, S., *et al*., EFFECTS OF DIETHOFENCARB ON THYROID FUNCTION AND HEPATIC UDP-GLUCURONYLTRANSFERASE ACTIVITY IN RATS. The Journal of Toxicological Sciences, 1992. 17(3): p. 155-16610.2131/jts.17.155 DOI|.
21. Jaiswal, S.K., N.J. Siddiqi, and B. Sharma, Carbofuran induced oxidative stress mediated alterations in Na+-K+-ATPase activity in rat brain: amelioration by vitamin E. Journal of biochemical and molecular toxicology, 2014. 28(7): p. 320-327
22. Hamed, H.S., S.M. Ismal, and C. Faggio, Effect of allicin on antioxidant defense system, and immune response after carbofuran exposure in Nile tilapia, Oreochromis niloticus. Comparative Biochemistry and Physiology Part C: Toxicology & Pharmacology, 2021. 240: p. 108919https://doi.org/10.1016/j.cbpc.2020.108919 DOI|.
23. Hernández-Moreno, D., *et al*., Brain acetylcholinesterase, malondialdehyde and reduced glutathione as biomarkers of continuous exposure of tench, Tinca tinca, to carbofuran or deltamethrin. Science of The Total Environment, 2010. 408(21): p. 4976-4983https://doi.org/10.1016/j.scitotenv.2010.07.044 DOI|.
24. Khalaf, A., Exploitation of Nano-Selenium Particles and Ionized Selenium for Attenuation the Hepatotoxicity and Nephrotoxicity Induced by Bisphenol A in Male Albino Rats. International Journal of Molecular Biology, ISSN, 2015: p. 0976-0482
25. Emara, S.S., Comparative Effects of Nano-Selenium and Sodium Selenite Supplementation on Blood Biochemical Changes in Relation to Growth Performance of Growing New Zealand White Rabbits. J Arab Journal of Nuclear Sciences, 2019. 52(4): p. 1-14

26. Arafa, M.H. and H.H. Atteia, Effect Of Selenium on Thyroid Biochemical and Histopathological Changes Induced by Subchronic Lead Acetate Exposure in Adult Albino Rats %J Mansoura Journal of Forensic Medicine and Clinical Toxicology. 2012. 20(2): p. 121-13810.21608/mjfmct.2012.47763 DOI|.

27. Hassanin, K.M., S.H. Abd El-Kawi, and K.S. Hashem, The prospective protective effect of selenium nanoparticles against chromium-induced oxidative and cellular damage in rat thyroid. Int J Nanomedicine, 2013. 8: p. 1713-2010.2147/ijn.S42736 DOI|.

28. Tang, J., *et al*., The clinicopathological significance of Ki67 in papillary thyroid carcinoma: a suitable indicator? World Journal of Surgical Oncology, 2018. 16(1): p. 10010.1186/s12957-018-1384-8 DOI|.

29. Hoffmann, P.R. and M.J. Berry, The influence of selenium on immune responses. Molecular nutrition & food research, 2008. 52(11): p. 1273-1280

30. Duntas, L.H., Environmental factors and autoimmune thyroiditis. Nature Clinical Practice Endocrinology & Metabolism, 2008. 4(8): p. 454-46010.1038/ncpendmet0896 DOI|.

الملخص العربى

آثار كريستالات جزيئات السيلينيوم النانوية (Cys Se-NPS) على التغيرات البيوكيميائية والتغيرات المناعية والبنية التحتية الدقيقة التي يسببها الكاربوفيوران في حصيلات الغدة الدرقية لدى ذكور الجرذان البيضاء البالغة.

سحر خليل[١]، أميمة محفوظ محمود[٢]، هالة محمد فتحي[٣،٤]، عبير عبد الخالق محمد[١]

[١]قسم الهستولوجي - كلية الطب - جامعة قناة السويس

[٢]قسم التشريح الأدمي وعلم الأجنة - كلية الطب - جامعة قناة السويس

[٣]قسم الفارماكولوجيا الأكلينيكية - كلية الطب - جامعة قناة السويس

[٤]المعمل المركزي، مركز التميز في الطب الجزيئي و الخلوي - كلية الطب - جامعة قناة السويس

مقدمة: كاربوفيوران مبيد حشري كرباماتي واسع االمجال يؤدي الي اضطراب الغدد الصماء و خاصه الغده الدرقيه تعتبر جزيئات السيلينيوم النانوية فعالة مثل السيلينيوم كعنصر نادر علي وظيفه الغده الدرقيه ولكن اقل في الخطوره.
هدف البحث: الهدف هو دراسة تأثير الحماية المحتمل لـ كريستالات جزيئات السيلينيوم النانوية على تلف الغدد الدرقية الناجم عن الكاربوفيوران.
مواد وأساليب العلاج: تم تقسيم أربعين من ذكور الجرذان البالغة عشوائياً إلى أربع مجموعات. مجموعة الضبط ، مجموعة الكربوفيوران: تم تلقي ٢,٤ ملغم / كغم من وزن الجسم من الكاربوفيوران. مجموعة الكاربوفيوران& كريستالات جزيئات السيلينيوم النانوية تلقت الكاربوفيوران كمجموعة سابقة بالإضافة إلى ٠,٣ ملغم / كغم من وزن الجسم كريستالات جزيئات السيلينيوم النانوية, مجموعة كريستالات جزيئات السيلينيوم النانوية:فقط تلقت كريستالات جزيئات السيلينيوم النانوية. تم تقييم تحليل المصل لهرمونات تي ٣ و تي ٤ وعلامات الأنسجة GSH و, MDA . تم تحضير أقسام الغدة الدرقية بسمك ٥ ميكرومتر ل صبغه الهيماتوكسولين، الميثون ثلاثية الألوان والكشف عن صبغه Ki٦٧ للأجسام المضادة المناعية. تمت معالجة عينات الغدة الدرقية الأخرى لفحصها بواسطة المجهر الإلكتروني النافذ.
النتائج: أظهرت مجموعة الكاربوفيوران انخفاضًا كبيرًا في جي اس اتش وكلا من تي ٣ و تي ٤ وزيادة مستوى MDA. كانت بصيلات الغدة الدرقية مشوشة ومدمرة بدرجة عالية ، مع ترقيم الخلايا الجريبية وزيادة ملحوظة في سمك الظهارة. تم الكشف عن الخلايا المقشرة في الغروانية مع انخفاض في حجمها. كشفت مجموعة الكاربوفيوران& كريستالات جزيئات السيلينيوم النانوية عن ارتفاع كبير في جي اس اتش و تي ٣ و تي ٤ وانخفاض مستوى ام دي ايه تم تحسين التشوهات النسيجية والبنية التحتية بشكل ملحوظ. تم تخفيض مؤشر ك اي ٦٧ بنسبة ٣,٦٩٪ مقارنة بـ ٦٢,٤٪ في مجموعة الكربوفيوران.
الاستنتاج: حسنت كريستالات جزيئات السيلينيوم النانوية التغييرات الناجمة عن الآثار السامة للكاربوفيوران والتي يمكن أن تكون علاجًا واعدًا ضد أنواع الأكسجين التفاعلية التي ينتجها الكربوفيوران.